Retinal Neurodegeneration in Type II Diabetic Otsuka Long-Evans Tokushima Fatty Rats

Ji Ho Yang,[1] Hyung Woo Kwak,[1] Tae Gi Kim,[1] Jisang Han,[1] Sang Woong Moon,[2] and Seung Young Yu[1]

[1]Department of Ophthalmology, Kyung Hee University Hospital, Kyung Hee University, Seoul, Korea
[2]Department of Ophthalmology, Kyung Hee University Hospital at Gangdong, Kyung Hee University, Seoul, Korea

Correspondence: Seung Young Yu, Department of Ophthalmology, Kyung Hee University Hospital, 23, Kyungheedae-ro, Dongdaemun-gu, Seoul, Republic of Korea; syyu@khu.ac.kr.

JHY and HWK contributed equally to the work presented here and should therefore be regarded as equivalent authors.

Submitted: November 15, 2012
Accepted: April 26, 2013

Citation: Yang JH, Kwak HW, Kim TG, Han J, Moon SW, Yu SY. Retinal neurodegeneration in type II diabetic Otsuka Long-Evans Tokushima fatty rats. *Invest Ophthalmol Vis Sci*. 2013;54:3844–3851. DOI:10.1167/iovs.12-11309

Purpose. We evaluated whether diabetes causes longitudinal thinning of retinal layers as a sign of retinal neurodegeneration in a type II diabetic animal model, the Otuska Long-Evans Tokushima fatty rats (OLETF), using spectral domain-optical coherence tomography (SD-OCT) and investigated the corresponding histology.

Methods. Retinal thickness in OLETF and Long-Evans Tokushima Otsuka rats (LETO) was measured at 1300 μm from the center of the optic nerve head (ONH) at 12, 20, 28, and 36 weeks using SD-OCT. Total retinal thickness (TRT) was measured automatically by built-in software. The retinal nerve fiber layer (RNFL) and other layers' thicknesses were measured manually. At 36 weeks, eyes were processed for morphometric analysis and detection of apoptosis based on active caspase-3$^+$ and TUNEL$^+$ analysis.

Results. TRT was significantly thinner in OLETF at 28 and 36 weeks (236.26 ± 5.64 and 235.98 ± 5.42 μm, respectively) than in LETO (243.82 ± 7.36 and 239.58 ± 6.99 μm, respectively; $P = 0.042$ and $P = 0.01$). At 28 weeks, RNFL thickness was significantly lower in OLETF (21.52 ± 1.91 μm) than in LETO (24.75 ± 2.10 μm, $P = 0.042$). The change of TRT correlated significantly with change of RNFL thickness. At 36 weeks, OLETF (24.0 ± 3.1/cross-section) had significantly fewer ganglion cells than LETO (28.4 ± 6.7/cross-section, $P = 0.028$). Active caspase-3$^+$ and TUNEL$^+$ cells in RNFL were observed significantly more frequently in OLETF (6.8 ± 5.2/cross-section and 3.75 ± 0.96/cross-section, respectively) than in LETO (1.5 ± 2.3/cross-section, $P = 0.008$ and 1.0 ± 0.8/cross-section, $P = 0.029$, respectively).

Conclusions. OLETF exhibited a significantly reduced TRT, especially RNFL thickness, based on SD-OCT. Further, histology revealed increased apoptosis and a decrease in the number of ganglion cells. These results suggest that retinal neurodegeneration occurs in type II diabetic OLETF.

Keywords: OLETF, neurodegeneration, diabetic retinopathy

Diabetic retinopathy (DR) is a microcirculatory disease of the retina caused by the deleterious effects of hyperglycemia and the metabolic pathways triggered by hyperglycemia. The vascular features of long-term DR are well documented.[1] Although DR leads to a progressive loss of visual function, little is known about the pathologic changes that occur in the retinal neurons.[2] Findings from electrophysiologic and electroretinogram (ERG) analyses suggest that DR involves the retinal neurons. Trick et al. reported changes in chromatic discrimination in 37% of diabetic patients with no vascular retinopathy and in 60% of patients with background retinopathy.[3] Feitosa-Santana et al. reported that only tritan losses in the D-15d test and diffuse loss in the Cambridge color test are observed before signs of retinopathy.[4] Frost-Larsen et al. reported that the oscillatory potential amplitude was reduced in patients with type I diabetes for 5 years before the development of vascular retinopathy.[5]

Early pathogenic mechanisms of DR were elucidated in animal models of diabetes and many attempts have been made to establish animal models that reflect the human condition accurately. Animal models used to investigate DR include streptozocin-induced diabetic rats and the spontaneously diabetic genetic model Ins2^{Akita} mouse.[6–8] Toxin-induced diabetes in rats has been less successful because of strain-dependent resistance to chemical toxins and toxic effects on neurons.[9,10] In addition, hyperglycemia is present in the streptozocin-induced diabetic and Ins2^{Akita} animal models, representing insulin-dependent diabetes. The general pathophysiology of these models is different from that of type II diabetes mellitus in humans. The Otsuka Long-Evans Tokushima Fatty rats (OLETF) suffer type II diabetes mellitus with metabolic syndrome, and the changes in the biologic characteristics of OLETF correspond to those of human type II diabetes mellitus,[6] including late onset hyperglycemia, chronic disease course, mild obesity, hyperplastic foci in pancreatic islets, later hypoinsulinemia as a result of deterioration of the islet beta cells, and retinal lesions.[11] Nearly 100% of male OLETF have diabetic mellitus via metabolic syndrome by 25 weeks of age.[11,12] Some studies have demonstrated the potential usefulness of an OLETF DR model. Maeda et al. reported that OLETF show changes in ERG in the early stages of hyperglycemia resembling those in human with diabetes mellitus.[13] Miyamura et al. reported that morphologic changes in the retinal capillaries of 14-month-

old OLETF were similar to those in diabetic patients.[14] Lu et al. reported changes that were similar to those of the retinal ultrastructure in patients with DR.[15]

In our study, we evaluated the longitudinal progressive thinning of retinal layers as a mark of retinal neurodegeneration in type II diabetic OLETF using spectral domain-optical coherence tomography (SD-OCT, Spectralis HRA+OCT; Heidelberg Engineering GmbH, Heidelberg, Germany) and investigated the corresponding histology.

Materials and Methods

Animals

OLETF were used in our study. OLETF and Long-Evans Tokushima Otsuka rats (LETO) were housed under standard conditions (12 h/d fluorescent light [7:00 AM–7:00 PM], 25°C room temperature) with free access to a commercial diet and water. Male LETO and OLETF were bred in the laboratory animal center at Kyung Hee University Hospital, according to the guidelines of Kyung Hee University Hospital Institutional Animal Care and Use, and the ARVO Statement for the Use of Animals in Ophthalmic and Vision Research. Only males were used in the present studies because disease progression in females is less uniform.[11] Age- and sex-matched nondiabetic LETO, obtained by different original matings from colonies of Long-Evans rats with OLETF, were used as controls. Body weight was measured bimonthly. Blood was obtained from tail veins, and an oral glucose tolerance test was performed in rats bimonthly at 12, 20, 28, and 36 weeks of age. Plasma glucose levels were determined using the glucose oxidase method with a free blood glucose meter and test strips (Accu-Check Active meter system; Roche Diagnostics Corporation, Indianapolis, IN). Diabetes mellitus was defined as having a peak plasma glucose level of more than 300 mg/dL or a plasma glucose level of higher than 200 mg/dL at 120 minutes in rats.[16]

Retinal Thickness

Before the eyes of OLETF and LETO were subjected to SD-OCT, the retinas were examined for evidence of gross pathology. There was no evidence of gross retinal disease in OLETF or LETO.

All rats were scanned using SD-OCT. Retinal nerve fiber layer (RNFL) circular scans centered at the optic disc were averaged automatically per B-scan to acquire the image at a constant distance from the optic disc. The "TruTracking Active Eye System" of the SD-OCT compensated for eye movements. The "AutoRescan" of SD-OCT enabled reacquisition of each OCT line actually captured in the baseline acquisition. Signal quality was greater than 25 dB and scan speed was 40,000 A-scans per second. Axial resolution was 7 μm optical and 3.5 μm digital.

Rats were anesthetized with an intramuscular injection of a Zoletil (200 mg/kg)/rompun mixture (50 mg/kg) and then placed on a positional stage. The head was fixed on a stabilizing bar. The eyes were dilated with topical tropicamide and small drops of methylcellulose (1%) were placed in the eye, followed by placement of a cover-slip and a double aspheric 60-D Volk lens (Volk Optical, Inc., Mentor, OH) to prevent corneal desiccation. We designed a new method to measure the thickness of various retinal layers using the "TruTracking Active Eye System" and "AutoRescan" of SD-OCT. Total retinal thickness (TRT) and other parameters in three regions of each eye were measured on a cross-sectional retinal image sampled along a 2600 μm diameter circle centered on the optic nerve head (ONH) using the RNFL circular scan (Fig. 1). Parameters measured in the selected scan included TRT, RNFL, inner plexiform layer (IPL), inner nuclear layer (INL), outer plexiform layer (OPL), and outer nuclear layer (ONL) thickness at 1300 μm from the center of the ONH. TRT was marked automatically by the segmentation software (Heidelberg Engineering GmbH) to delineate the internal limiting membrane and RPE-Bruch's membrane, and then the distance between them was obtained in almost all rats. Cases with failed segmentation of the TR due to poor resolution of the acquired OCT images and other layer borders were corrected manually by two experienced assistants at each follow-up examination.

Intrasession variability was determined by calculating the coefficient of variance (CV) of the thickness obtained in three successive images.

Histology

Immediately after 36 weeks, the OLETF ($n = 28$ eyes) and age-matched LETO ($n = 38$ eyes) were killed, and their eyes enucleated. To evaluate the histologic characteristics of OLETF and LETO retinas, fixation, hematoxylin and eosin (H&E) staining, and immunofluorescence were performed as reported previously.[6] For studies using frozen sections, eyes were enucleated and imbedded in optimal cutting temperature compound (OCT, Tissue Tek; Miles Laboratories, Elkhart, IN) so that 14 μm thick sections included the full length of the retina along the horizontal meridian, passing through the ora serrata and optic nerve in the temporal and nasal hemispheres. The eyes were flash frozen, and cryosections were prepared and mounted on slides. Sections were stained with H&E and used for morphologic studies. The number of ganglion cells in the RNFL of OLETF and LETO was determined in two peripheral regions of each section on either side at 1300 μm from the ONH under light microscopy using ×200 and ×400 magnification. The number of retinal ganglion cells was counted manually in cross-sections from each rat eye per 1750 μm length of retina. Additional immunofluorescence methods were performed on cryosections for the detection of active caspase-3 (Cell Signaling Technology, Inc., Beverly, MA) and TUNEL analysis (Trevigen, Inc., Gaithersburg, MD) per 750 μm length of retina. Tissues were viewed by epifluorescence using standard fluorescence excitation and emission filters with a fluorescent microscope (Olympus BX 51; Olympus Optical Co., Ltd., Tokyo, Japan) at ×200 and ×400 magnification.

Statistical Analysis

Statistical comparisons were performed using SPSS 12.0 (SPSS, Inc., Chicago, IL). A paired *t*-test was performed to analyze the various retinal thickness changes compared to baseline values and to analyze the various retinal thickness changes over time. An independent *t*-test was performed to compare the various retinal thicknesses at 12, 20, 28, and 36 weeks, and the number of ganglion cells and active caspase-3$^+$ cells at 36 weeks between LETO and OLETF. A Mann-Whitney *U* test was performed to compare TUNEL$^+$ cells at 36 weeks between LETO and OLETF.

Intrasession repeatability was assessed based on the CV. We evaluated changes in the TRT at follow-up as the dependent variables, including RNFL, IPL, INL, ONL, and OPL in OLETF from 12 to 36 weeks with multiple linear regression analysis. A P value of less than 0.05 was considered statistically significant.

Results

Body Weight and Blood Glucose Level

OLETF gained weight faster than LETO. The difference increased gradually between LETO and OLETF until 36 weeks (36 weeks, 457 g in OLETF and 338 g in LETO, $P < 0.005$).

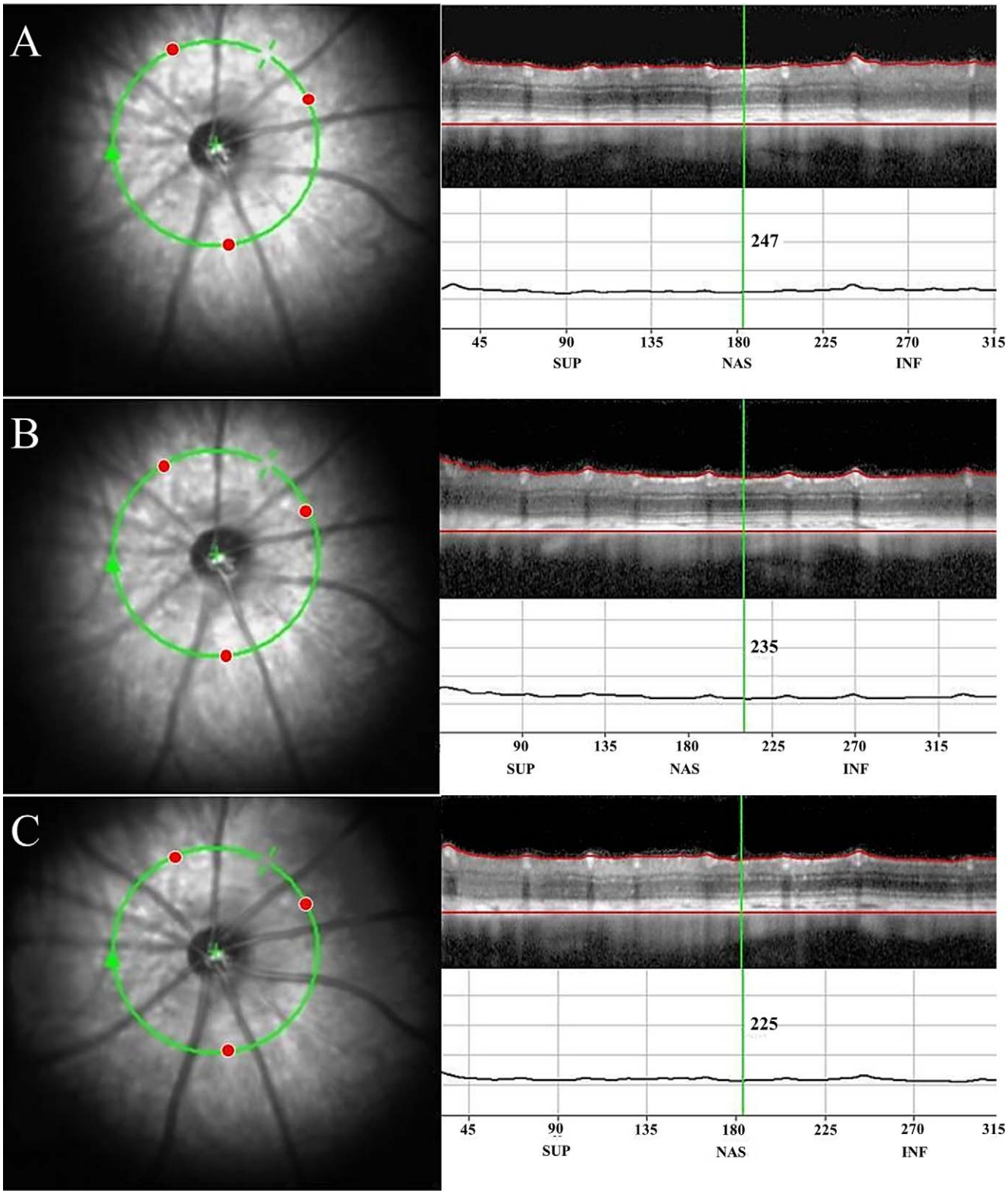

Figure 1. IR fundus photograph, OCT, and retinal thickness map. The *green ring line* in the IR fundus photograph indicates the position of the RNFL circular scan. The B-scan demonstrates autosegmentation of the inner limiting membrane (*upper red line*) and RPE-Bruch's membrane (*lower red line*). Retinal thickness map shows TRT (**A**) at 12 weeks, (**B**) at 28 weeks, and (**C**) at 36 weeks with AutoRescan. *Red circle*: check point for retinal thickness.

Investigative Ophthalmology & Visual Science

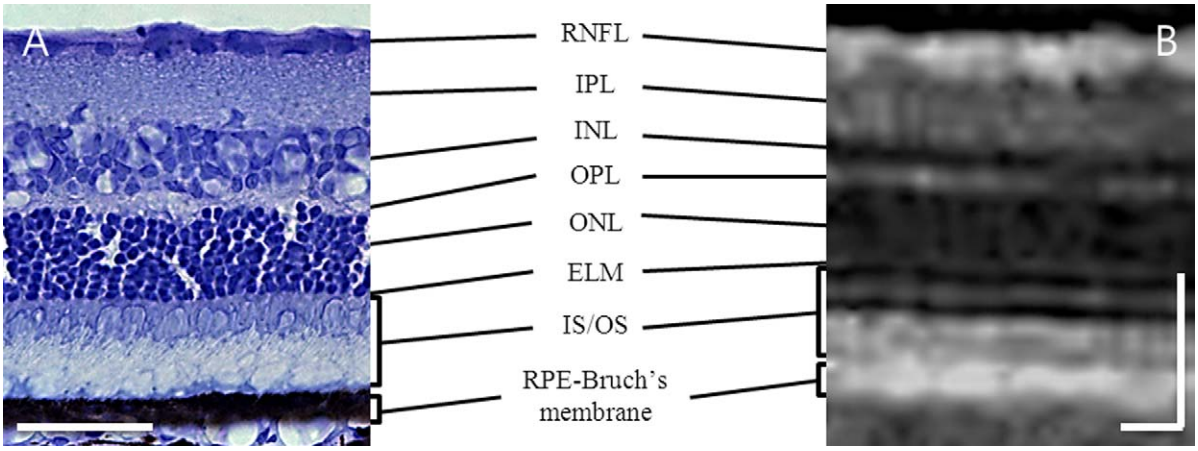

FIGURE 2. Comparison of the histologic image (**A**) with the OCT cross-sectional image (**B**) of LETO retina. All intraretinal layers are observed in the OCT image. ELM, external limiting membrane; IS/OS, the inner and outer segments of the photoreceptors; RPE-Bruch's membrane. *Scale bar*: 100 μm.

Blood glucose levels were higher in OLETF than in LETO beginning at 20 weeks, and remained higher at 36 weeks (36 weeks, 327.9 mg/dL in OLETF and 145.9 mg/dL in LETO, $P < 0.05$).

OCT Imaging of Rat Retina

Infrared reflectance (IR) fundus image shows that follow-up scan was placed precisely in the same location as previously. Changes in retinal thickness were observed in the same location of the retina during follow-up (Fig. 1). Retinal thickness map shows TRT 247 μm at 12 weeks (Fig. 1A), 235 μm at 28 weeks (Fig. 1B), and 228 μm at 36 weeks at the red circle in Figure 1C.

We identified individual retinal layers in SD-OCT images (Fig. 2B) by comparing them with histologic images (Fig. 2A) obtained from the same retina. The SD-OCT image shows all the anatomic retinal layers are in good correlation with histology. The OCT image is displayed in gray scale, with darker areas corresponding to lower backscattering and brighter ones representing higher backscattering.

The OCT image of rat retina is qualitatively similar to that of the human retina.[17,18] RNFL or plexiform layers are optically backscattering, whereas nuclear layers are weakly backscattering. The OCT image delineated the inner retinal border (internal limiting membrane) between the nonreflective vitreous and the backscattering retina. The RNFL represents the first layer in the OCT images, with relatively high backscattering, and can be distinguished as a bright band at the top of the OCT image. Further down in the retina, bands of relatively high and low backscattering are observed, and they correspond to the IPL, INL, OPL, and ONL, respectively.

Retinal Thickness

We used SD-OCT to measure TRT, RNFL, IPL, INL, OPL, and ONL thickness. At 28 and 36 weeks, the TRT in OLETF (28 weeks, 236.26 ± 5.64 μm and 36 weeks, 235.98 ± 5.42 μm) was significantly thinner than that in LETO (28 weeks, 243.82 ± 7.36 μm, $P = 0.042$ and 36 weeks, 239.58 ± 6.99 μm, $P = 0.01$) in Figures 3A, 3G, and 3H. RNFL thickness was significantly thinner in OLETF (28 weeks, 21.52 ± 1.91 μm and 36 weeks 21.08 ± 1.94 μm) than that in LETO (28 weeks, 24.75 ± 2.10 μm, $P = 0.042$ and 36 weeks, 24.37 ± 2.02 μm, $P = 0.01$) in Figures 3B, 3G, and 3H. TRT and RNFL thickness decreased gradually for up to 20 weeks, and then dropped suddenly at 28 weeks in OLETF in Figures 3A and 3B. TRT and RNFL thickness decreased gradually for up to 36 weeks in LETO in Figures 3A and 3B.

IPL, INL, OPL, and ONL thicknesses did not differ significantly between OLETF and LETO (Figs. 3C–F).

The decrease in the TRT could be caused by changes in the thickness of the various retinal layers. To differentiate between these possibilities, we performed a multiple linear regression analysis with change in TRT at follow-up as the dependent variables. Significant positive correlations were found between change in the TRT and RNFL ($r = 0.435$, $P = 0.049$), and between changes in TRT and IPL ($r = 0.444$, $P = 0.036$). There was no significant correlation between TRT and other variables, such as INL, OPL, and ONL.

Intrasession variability in the TRT, and RNFL, IPL, INL, OPL, and ONL thickness was 4.8%, 5.1%, 5.9%, 8.4%, 7.8%, and 5.5%, respectively.

Histology

H&E-stained sections of LETO and OLETF retina at 36 weeks are shown in Figures 4A and 4B. Ganglion cells in OLETF were not distributed uniformly, suggesting cellular dropout in the RNFL. In contrast, ganglion cells in LETO were densely packed and uniformly distributed. Except for occasional blood vessels, there was little space between cells. The RNFL had significantly fewer ganglion cells in OLETF (24.0 ± 3.1/cross-section) compared to LETO (28.4 ± 6.7/cross-section, $P = 0.028$, $n = 10$ per group, Fig. 4G).

To characterize the cell loss observed in the RNFL of OLETF, we performed the TUNEL analysis to detects cells with fragmented DNA and, though used widely as a marker for apoptosis, also reflects cells dying by necrosis[6] and levels of active caspase-3, an apoptosis marker,[19] as an assay of cell death. Significantly more active caspase-3$^+$ cells were observed in the RNFL of OLETF (6.8 ± 5.2/cross-section) than in LETO (1.5 ± 2.3/cross-section, $P = 0.008$, $n = 10$ per group) in Figure 4H. Significantly more TUNEL$^+$ cells were observed in the RNFL in OLETF (3.75 ± 0.96/cross-section) than in LETO (1.0 ± 0.8/cross-section, $P = 0.029$, $n = 4$ per group, Fig. 4I). Photomicrographs of retinas processed for active caspase-3 and TUNEL analysis are shown in Figures 4C to 4F.

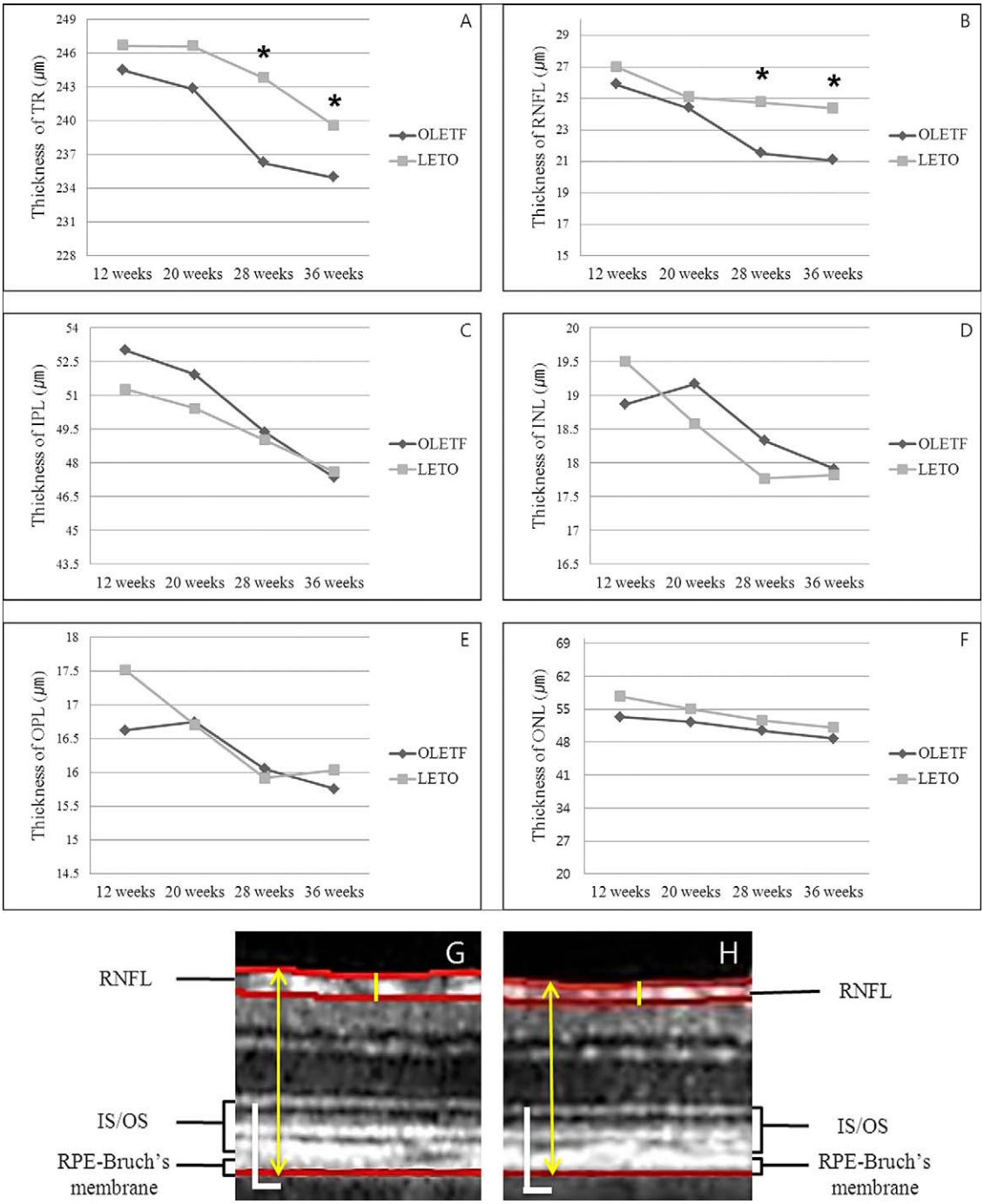

Figure 3. Graphs show changes in the thickness of each retinal layer of the OLETF and LETO. (**A**) Changes in TRT over 36 weeks. (**B**) Changes in the RNFL. (**C**–**F**) Changes in the thickness of the IPL, INL, OPL, and ONL. Each of the four layers showed a similar pattern at different experimental time-points, indicating a slight decrease. For confirmation and comparison in (**A**, **B**), (**G**) shows an OCT image at 1300 μm inferior to the center of the ONH in LETO. (**H**) shows an OCT image at 1300 μm inferior from center of the ONH in OLETF. Data are the means of measurements in retinas of 28 eyes from OLETF and 38 eyes from LETO. *Significantly different from control ($P < 0.05$). *Scale bar*: 100 μm.

Discussion

In our study, we investigated in vivo changes in retinal thickness over time in type II diabetic OLETF to evaluate retinal neurodegeneration using SD-OCT and related the histology to changes in retinal thickness.

We designed a new method to measure various retinal thicknesses with SD-OCT. Measuring the thicknesses of the various retinal layers with SD-OCT has several important advantages over conventional histology. First, SD-OCT allows for noninvasive in vivo examination of the retina in live animals, which is key to performing longitudinal studies. It is difficult to monitor retinal thickness with conventional histology without killing the animal. Histologic methods are limited to follow-up of disease progression. Second, SD-OCT excludes the bias from thickness measurements of various retinal layers and inherent artifacts in histologic preparation, including tissue shrinkage from fixation and compression, and

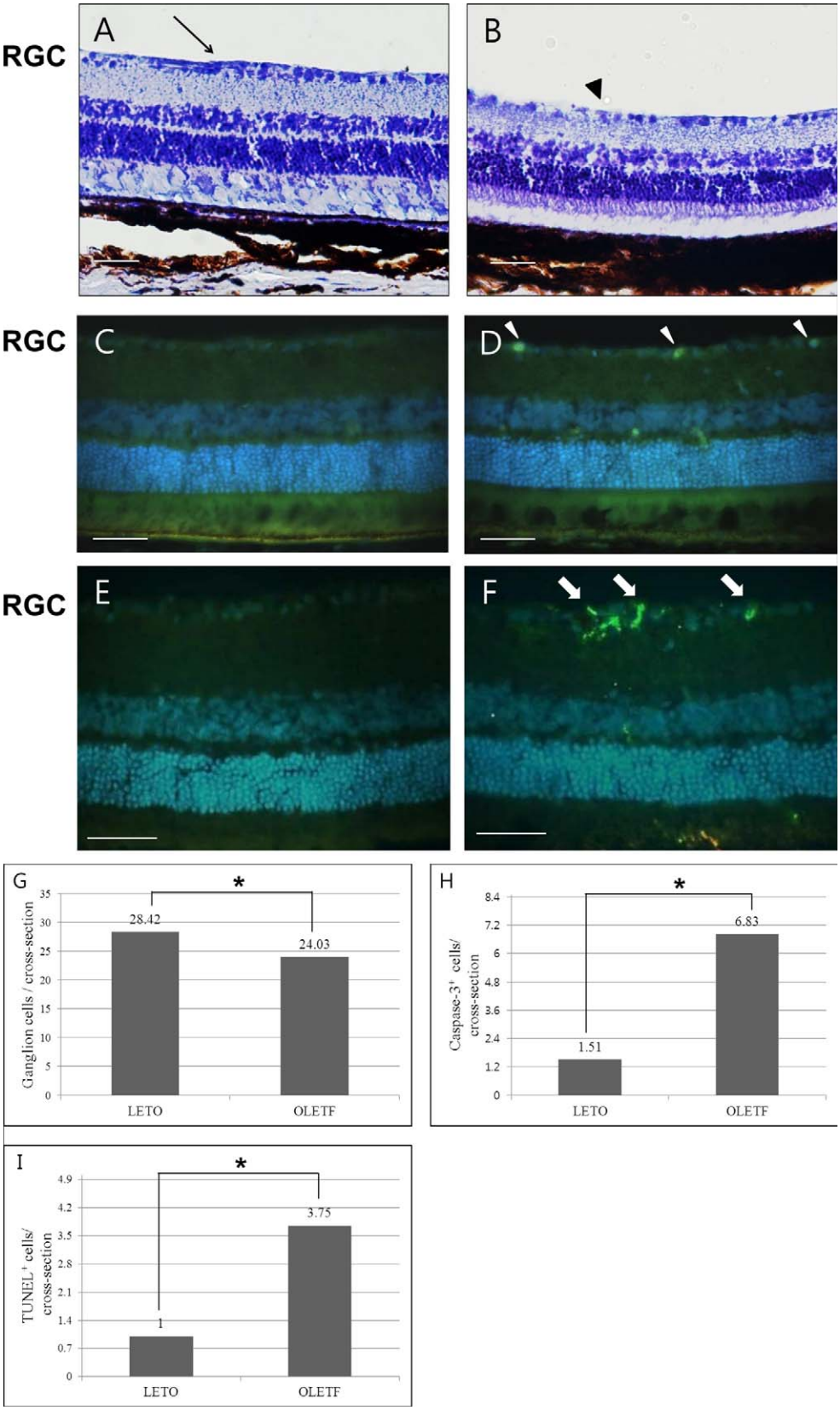

Figure 4. Light microscopic evaluation of OLETF and age-matched nondiabetic LETO retina at 36 weeks. H&E-stained cryosections of the retina of LETO (**A**) and OLETF (**B**). The cells of the RNFL are distributed uniformly in the LETO (*arrow*), whereas there are areas of cellular dropout in OLETF retina (*black arrowhead*). Fluorescence microscopic detection of active caspase-3 in retinas of LETO (**C**) and OLETF (**D**). Fluorescence microscopic detection of TUNEL analysis in retinas of LETO (**E**) and OLETF (**F**). Number of cells in the RNFL of LETO and OLETF (**G**). Number of active caspase-3$^+$ (**H**) and TUNEL$^+$ (**I**) cells in the RNFL of LETO and OLETF. *Blue fluorescent signal*: nuclei of all cells stained with 4′,6′-diamino-2-phenylindole (DAPI). *Green signal*: cells for active caspase-3$^+$ (*white arrowheads*) and TUNEL$^+$ (*white arrows*). *Significantly different from control ($P < 0.05$). Magnification: ×200 and ×400. *Scale bar*: 100 μm.

oblique sections cut during sectioning.[20,21] Third, SD-OCT has faster scanning rates and higher axial resolution, allowing for the acquisition of detailed microstructures in rodents.[17,22] Fourth, SD-OCT allows for acquisition of the same image as previous scan images during the follow-up period with built-in software. We used the "TruTraking Active Eye System" of SD-OCT, which compensates for eye movements during breathing and blinking. It is difficult to find a specific location on the retina due to the large number of vessels and the lack of a specific landmark, excluding the optic disc (hyaloid stalk), when the retina of rats is rescanned using the vertical plane scan of OCT. We used the AutoRescan and RNFL circular scan of the SD-OCT to measure retinal thickness. The AutoRescan of SD-OCT can identify previous scan locations and guide the OCT laser to scan the same location, and, therefore, has a follow-up function to ensure that the same scanning location is identified on subsequent examinations. It is difficult to perform an AutoRescan because the AutoRescan can acquire an image to alignment currently image location from a previous acquired image, such as many vessels and scanned location. To solve this problem and measure the same location measured previously, we performed the RNFL circular scan to measure a constant distance from the optic disc using the AutoRescan. Measuring retinal thickness with SD-OCT, however, has several limitations. The lateral magnification of the rat fundus should be approximately five times larger than that of the human fundus, according to data of representative rat[23] and human eyes (Gullstrand's schematic eye), the axial length of a rat eye is much shorter than that of humans (6.92 vs. 24.00 mm), and total power of the rat eye is much greater than that of human eye (300.705 vs. 58.64)[20,24] To address the limitations of using OCT, we obtained an image toward the center position rather than to one side, and applied hydroxypropyl methylcellulose and a cover slip to negate the refractive power of the cornea.

Our results suggested that neurodegeneration occurs predominantly in the RNFL after 28 weeks (approximately 8 weeks after the development of diabetes) in OLETF due to DR. These data are consistent with previous data regarding retinal thickness in diabetes. Martin et al. reported that TRT, INL, and ONL were decreased in mice within 10 weeks after the development of diabetes.[6] Barber et al. reported a significant reduction in the thickness of the TR, IPL, INL, and the number of ganglion cells in streptozocin diabetic rats compared to controls.[2] Barber et al. reported significant reductions in the thickness of the IPL and INL in diabetic mice compared to controls within 22 weeks after hyperglycemia.[7] Park et al. reported a slight reduction in the thickness of the inner retina and a marked reduction in the thickness of the ONL at 24 weeks after the onset of diabetes.[8] Together, these data indicate that retinal thickness is decreased in diabetic rats. There are, however, subtle differences in the decreases of the retinal layer thicknesses. The reason for these differences is unclear, but the inconsistency might be due to differences in species and the methods used to induce diabetes.

In our study, the thickness of various retinal layers decreased over time, and there were no differences in the thickness of any of the layers between OLETF and LETO until 20 weeks (Fig. 3). Thickness was decreased at 20 weeks in both groups and continued to decrease in LETO up to 36 weeks, although less than that in OLETF, consistent with previously reported age-related changes in the rat retina.[25]

We performed histology to confirm the results of the SD-OCT. Based on the number of neurons in the RNFL, a significant loss of ganglion cells in the RNFL was observed in OLETF compared to LETO. This finding is consistent with previous data regarding the number of ganglion cells in diabetic rodents. Martin et al. reported that within approximately 10 to 14 weeks after the onset of diabetes, there were significantly fewer cells in the ganglion cell layer in diabetic mice than in age-matched nondiabetic mice.[6] Barber et al. reported a 23.4% reduction in the number of cell bodies in the retinal ganglion cell layer in diabetic mice.[7]

In our study, the decrease in TRT and RNFL thickness, and the decrease in the number of retinal ganglion cells in OLETF suggested neuronal cell loss in the RNFL. Based on an apoptotic assay, neurons of the RNFL in OLETF were dying by apoptosis. The apoptotic cells were identified by immunofluorescence with an antibody that recognizes the active form of caspase-3 and TUNEL analysis. We used 14 μm thick cryosections to detect active caspase-3$^+$ and TUNEL$^+$ cells. In these cryosections, it was clear that ganglion cells of the RNFL were affected. The assay results revealed significantly more active caspase-3$^+$ and TUNEL$^+$ cells in the RNFL of OLETF than in the RNFL of LETO. Barber et al. reported a 10-fold increase in retinal apoptosis of retinal ganglion cells after 12 months of diabetes.[2] Asnaghi et al. reported a 4-fold increase in apoptotic neurons in streptozocin-induced diabetic rats compared to nondiabetic rats.[26]

Neurodegeneration leads to changes of ERG in DR. Shinoda et al. reported that implicit times of oscillatory potentials were significantly longer in diabetic rats 1 month after streptozocin treatment.[27] Li et al. reported that diabetic rats have reduced ERG responses as early as 2 weeks after the onset of diabetes.[28] Segawa et al. suggested that retinal neuronal dysfunction revealed by oscillatory potential abnormalities in the ERG occurred before the angiopathic diabetic changes in OLETF.[29] It is expected that the change in the ERG response will correlate with reduced ganglion cell counts. Our study is limited in that these findings are not complemented by functional data corresponding to decreased retinal thickness and increased apoptosis. Functional studies, such as ERG, would be performed in conjunction with histologic and OCT studies in future investigations. However, a major strength of our study is the finding that structural changes characterized by longitudinal in vivo measurement can be a biomarker for assessing retinal neurodegeneration.

We did not attempt to determine the mechanism of neurodegeneration in OLETF. Recent studies reported increased levels of glutamate in the vitreous of rats with diabetes.[30,31] Villarroel et al. reported that overexpression of the renin–angiotensin system has an essential role in neurodegenerative processes in the diabetic retina.[10] Park et al. reported that diabetes upregulates the expression of neuronal nitric oxide synthase in bipolar cells, and nitric oxide from these cells may aggravate degeneration of the outer retina in diabetic retinas.[32] Further attempts to understand the mechanisms and mediators of neurodegeneration in DR in OLETF, and to develop treatments for this disease will require consideration of the roles and interactions of all three cellular elements (neuronal, glial, and vascular cells).

Several studies have examined whether DR is a result of neurodegeneration,[2] microangiopathic changes,[33] or both.[7] The neurodegenerative and microangiopathic changes are likely to be closely linked components of DR.[34] Barber proposed two possible explanations to account for the relation between the neurodegenerative and microangiopathic changes.[34] First, loss of the blood–retinal barrier integrity, which initially manifests as an increase in vascular permeability, leads to a failure to control the composition of the extracellular fluid in the retina, which results in edema and neuronal cell loss. Alternatively, diabetes directly affects metabolism within the neural retina, which leads to an increase in apoptosis and causes a breakdown of the blood–retinal barrier. The intimate relationship between the neurodegenerative and microangiopathic changes, however, is not clear at cellular level. Further investigation of the relationship between the neurodegenera-

tion and microangiopathic changes is needed to elucidate the mechanisms of DR and to develop applicable therapies.

In conclusion, TRT and RNFL thickness begin to decrease in OLETF after 28 weeks with SD-OCT. Ganglion cells decrease and apoptotic cells are detected in the RNFL at 36 weeks through histology. Our results suggest that sustained retinal neurodegeneration in type II diabetic OLETF begins after 28 weeks.

Acknowledgments

The authors alone are responsible for the content and writing of the paper.

Disclosure: **J.H. Yang**, None; **H.W. Kwak**, None; **T.G. Kim**, None; **J. Han**, None; **S.W. Moon**, None; **S.Y. Yu**, None

References

1. Engerman RL, Kern TS. Retinopathy in animal models of diabetes. *Diabetes Metab Rev*. 1995;11:109–120.
2. Barber AJ, Lieth E, Khin SA, Antonetti DA, Bchanan AG, Gardner TW. Neural apoptosis in the retina during experimental and human diabetes. *J Clin Invest*. 1998;102:783–791.
3. Trick GL, Burde RM, Gordon MO, Santiago JV, Kilo C. The relationship between hue discrimination and contrast sensitivity deficits in patients with diabetes mellitus. *Ophthalmology*. 1998;95:693–698.
4. Feitosa-Santana C, Paramei GV, Nishi M, Gualtieri M, Costa MF, Ventura DF. Color vision impairment in type 2 diabetes assessed by the D-15d test and Cambridge colour test. *Ophthalmic Physiol Opt*. 2010;30:717–723.
5. Frost-Larsen K, Larsen HW, Simonsen SE. Oscillatory potential and nyctometry in insulin-dependent diabetics. *Acta Ophthalmol*. 1980;58:879–888.
6. Martin PM, Roon P, Smithe SB, Ganapathy V, Van Ells TK. Death of retinal neurons in streptozocin-induced diabetic mice. *Invest Ophthalmol Vis Sci*. 2004;45:3330–3336.
7. Barber AJ, Antonetti DA, Kern TS, et al. The Ins2Akita mouse as a model of early retinal complications in diabetes. *Invest Ophthalmol Vis Sci*. 2005;46:2210–2218.
8. Park SH, Park SJ, Kim KY, Chung JW, Oh SJ. Apoptotic death of photoreceptors in the streptozotocin-induced diabetic rat retina. *Diabetoglia*. 2003;46:1260–1268.
9. Rossini AA, Appel MC, Williams RM, Like AA. Genetic influence of the streptozocin-induced insulinitis and hyperglycemia. *Diabetes*. 1977;26:916–920.
10. Villarroel M, Ciudin A, Hernandez C, Simo R. Neurodegeneration: an early event of diabetic retinopathy. *World J Diabetes*. 2010;15:57–64.
11. Kawano K, Hirashima T, Moris S, Saito Y, Kurosumi M, Natori T. Spontaneous long-term hyperglycemic rat with diabetic complications: Otsuka Long-Evans Tokushima Fatty (OLETF) strain. *Diabetes*. 1992;41:1422–1428.
12. Nagai N, Murao T, Ito Y, Okamoto N, Okamura H. Involvement of interleukin 18 in lens opacification of Otsuka Long-Evans Tokushima Fatty rats, a model of human type 2 diabetes. *Curr Eye Res*. 2011;36:497–506.
13. Maeda K, Segawa Y, Asai H, Shirao Y, Sounou T, Yamada A. Changes in electroretinograms of spontaneously diabetic rats. *Folia Ophthalmol Jpn*. 1997;48:851–854.
14. Miyamura N, Bhutto IA, Amemiya T. Retinal capillary changes in Otsuka Long-Evans Tokushima Fatty Rats (spontaneously diabetic strain). *Ophthalmic Res*. 1999;31:358–366.
15. Lu ZY, Bhutto IA, Amemiya T. Retinal changes in Otuska Long-Evans Tokushima Fatty rats (spontaneously diabetic rat)-possibility of a new experimental model for diabetic retinopathy. *Jpn J Ophthalmol*. 2003;47:28–35.
16. Hirashima T, Kawano K, Mori S, Matsumoto K, Natori T. A diabetogenic gene (0DB-1) assigned to the X-chromosome in OLETF rats. *Diabetes Res Clin Pract*. 1995;27:91–96.
17. Ruggeri M, Webbe H, Jiao S, et al. In vivo three-dimensional high-resolution imaging of rodent retina with spectral-domain optical coherence tomography. *Invest Ophthalmol Vis Sci*. 2007;48:1808–1814.
18. Lozano DC, Twa MD. Quantitative evaluation of factors influencing the repeatability of SD-OCT thickness measurements in the rat. *Invest Ophthalmol Vis Sci*. 2012;53:8378–8385.
19. Kieckle FL, Zhang Z. Apoptosis: biomechanical aspects and clinical implications. *Clin Chim Acta*. 2002;326:27–45.
20. Nagata A, Higashide T, Ohkubo S, Takeda H, Sugiyama K. In vivo quantitative evaluation of the rat retinal nerve fiber layer with optical coherence tomography. *Invest Ophthalmol Vis Sci*. 2009;50:2809–2815.
21. Margo CE, Lee A. Fixation of whole eyes: the role of fixative osmolarity in the production of tissue artifact. *Graefes Arch Clin Exp Ophthalmol*. 1995;233:366–370.
22. Garbriele ML, Ishikawa H, Schuman JS, et al. Reproducibility of spectral-domain optical coherence tomography total retinal thickness measurements in mice. *Invest Ophthalmol Vis Sci*. 2010;51:6519–6523.
23. Hughes A. A schematic eye for the rat. *Vision Res*. 1979;19:569–588.
24. Kawaguchi I, Higashide T, Ohkubo S, Takeda H, Sugiyama K. In vivo imaging and quantitative evaluation of the rat retinal nerve finer layer using scanning laser ophthalmoscopy. *Invest Ophthalmol Vis Sci*. 2006;47:2911–2916.
25. Cavallotti C, Artico M, Pescosolido N, Fehe J. Age-related changes in rat retina. *Jpn J Ophthalmol*. 2001;45:68–75.
26. Asnaghi V, Gerhardinger C, Hoehn T, Adeboje A, Lorenzi M. A role for the polyol pathway in the early neuroretinal apoptosis and glial changes induced by diabetes in the rat. *Diabetes*. 2003;52:506–511.
27. Shinoda K, Reidak R, Schuettauf F, et al. Early electroretinographic features of streptozocin-induced diabetic retinopathy. *Clin Experiment Ophthalmol*. 2007;35:847–854.
28. Li Q, Zemel E, Miller B, Perlman I. Early retinal damage in experimental diabetes: electroretinographical and morphological observations. *Exp Eye Res*. 2002;74:615–25.
29. Segawa Y, Shirao Y, Yamagishi S, et al. Upregulation of retinal vascular endothelial growth factor mRNAs in spontaneously diabetic rats without ophthalmoscopic retinopathy. A possible participation of advanced glycation end products in the development of the early phase of diabetic retinopathy. *Ophthalmic Res*. 1998;30:333–339.
30. Lieth E, Barber AJ, Xu B, et al. Glial reactivity and impaired glutamate metabolism in short-term experimental diabetic retinopathy. *Diabetes*. 1998;47:815–820.
31. Kowluru RA, Engerman RL, Case GL, Kern TS. Retinal glutamate in diabetes and effect of antioxidants. *Neurochem Int*. 2001;38:385–390.
32. Park JW, Park SJ, Park SH, et al. Up-regulated expression of neuronal nitric oxide synthase in experimental diabetic retina. *Neurobiol Dis*. 2006;21:43–49.
33. Feit-Leichman RA, Kinouchi R, Takeda M, et al. Vascular damage in a mouse model of diabetic retinopathy: relation to neuronal and glial changes. *Invest Ophthalmol Vis Sci*. 2005;46:4281–4287.
34. Barber AJ. A new view of diabetic retinopathy: a neurodegenerative disease of the eye. *Prog Neuropsychopharmacol Biol Psychiatry*. 2003;27:283–290.